JurnalPolimesin
Department of Mechanical Engineering
State Polytechnic of Lhokseumawe
http://e-jurnal.pnl.ac.id/polimesin
e-ISSN : 2549-1999 No. : 2 Month : April
p-ISSN : 1693-5462 Volume : 22 Year : 2024

Article Processing Dates: Received on 2023-08-17, Reviewed on 2023-09-07, Revised on 2024-01-03, Accepted on 2024-03-07 and Available online on 2024-04-30

Real-time thermodynamic monitoring of split inverter ACs: a microcontroller-driven investigation of performance

I Gede Artha Negara*, Adi Winarta, PutuWijayaSunu, I Dewa Made Cipta Santosa, I Nyoman Suamir, I Gusti Agung Bagus Wirajati, I Dewa Gede Agus Tri Putra
Mechanical Engineering Department, Bali State Polytechnic, Bukit Jimbaran, 80364, Indonesia
*Corresponding author: artha_negara@pnb.ac.id

Abstract

Recent technological advancements, particularly in air conditioning cooling systems, have led to rapid developments such as inverter technology. Inverter technology provides various advantages including energy savings compared to non-inverter air conditioners. Globally, the inverter modulates the compressor to continue operation despite reaching the set temperature. This study aimed to monitor the performance of split inverter air conditioners utilizing microcontroller technology. The microcontroller model employed was the ATmega 2560, capable of logging each test parameter and displaying in real-time. Additionally, the ATmega 2560 integrated sensors including the DS18B20 temperature sensor and PZEM 004-T multifunction electrical sensor. Monitoring occurred over one hour of operation on a 2.5 kW capacity split inverter AC. The experimental monitoring results show that the minimum temperature was recorded at T_{supply} in comparison to the other temperature points. $T_{supply}$was found to attain a temperature of 8°C during the investigation. The findings for T_{return} exhibit a similar declining trend, with the temperature reaching 25.5°C at approximately 3000 s. The lowest power fluctuations were observed at the remote temperature of 24°C compared to other remote temperatures. The average power consumption of the split inverter AC was approximately 750 W. Peak energy consumption was observed at 0.96 kWh during one hour of operation of the split inverter AC. Microcontroller-based experimental monitoring can provide real-time results and shows promise for monitoring split inverter AC performance.

Keywords:
Air conditioning cooling system, thermodynamic, microcontroller, performance, real-time.

1 Introduction

In recent years, advanced Air conditioning (AC) technologies such as inverters have been developed [1]–[3]. Inverters are devices that can change the frequency of the AC power supply. Inverter AC systems operate the compressor at variable speeds rather than binary on/off [4]–[6]. This inverter technology enables modulation of the compressor operation and helps control energy consumption compared to non-inverter ACs. Inverter ACs can achieve target temperatures faster than conventional ACs. The performance of an AC system depends on various factors including ambient temperature, cooling load, and system condition [7]. These factors affect the cooling capacity and room comfort [8]–[10]. Per AC design standards, the evaporator temperature difference should be at least 8°C. However, lower temperature differences may indicate issues with the AC system[11].

Power consumption of an air conditioner can be determined from measurements of current and voltage. Investigating the performance of an air conditioner requires measurement of parameters including evaporator, compressor, and condenser temperatures [12], [13]. Additionally, the electrical performance should be characterized by measuring current, voltage, power, frequency, and energy usage [14]. To obtain accurate investigative results, microcontroller technology can be utilized. A microcontroller is an integrated circuit containing a processor, memory, and input/output peripherals designed to govern a specific operation in an embedded system [15], [16]. Microcontrollers are commonly found in diverse applications including vehicles, robots, medical devices, and home appliances [17]. Advantages of microcontrollers include real-time data acquisition, rapid operation, compact and adaptable hardware, and cost-effectiveness [18], [19]. For air conditioner investigations, microcontrollers can interface with various sensors such as temperature, humidity, and voltage probes. This microcontroller enables integrated monitoring of investigative results.

Previous investigations of residential air conditioning systems have been carried out. Sumeru et al. [20] discussed an experimental investigation on the use of water condensate to improve the performance of residential air conditioning systems. Experimental results demonstrate the application of condensate water decreases refrigerant temperature at the condenser outlet by 2.7°C. This corresponds to a 16.4% increase in the Coefficient of Performance (COP) of the system. Furthermore, the condensate water reduces compressor discharge temperature by 7.6°C, corresponding to a 5.9% reduction in power consumption. The novelty of the research lies in the experimental investigation conducted to explore the use of condensate water as a discharge cooler to enhance the performance of residential air conditioning systems. This study specifically focuses on lowering the temperature of the compressor discharge, which results in subcooling and subsequently improves the cooling capacity of the system. Overall, the exploitation of waste condensate water for subcooling substantially improves the thermodynamic efficiency and cooling capacity of the air conditioning system.

Deng et al. [21] examined the influence of air conditioner operation on energy consumption and savings in a modeled building with varying exterior wall thermal insulation types. The novelty of the research lies in its investigation of the impact of air conditioner operation on energy consumption in residential buildings with varying types of exterior wall insulation. This study emphasizes the influence of human thermal experience on AC operation behavior, high lighting how indoor temperature deviations affect operation frequencies. Additionally, the comparison between continuous and intermittent energy usage modes reveals insights into the effectiveness of various insulation types. Results demonstrate air conditioner operational behavior is contingent on indoor temperature and human thermal comfort. Additionally, comparative analyses of energy savings from interior and exterior thermal insulation are presented under diverse operational schemas. The investigative outcomes quantify the impacts of insulation selection and air conditioner operating conditions on building energy performance. Ren and Cao [22] examined the maturation and employment of linear ventilation and thermal archetypes for indoor ambiance prognostication and HVAC framework regulation. The objective of the inquiry is to furnish enhanced control methodologies for Heating, Ventilation, and Air Conditioning (HVAC) arrangements to provide occupancy-actuated energy and comfort stewardship. The examination implements low-dimensional linear exemplars, artificial neural lattices, and donation ratios of indoor atmosphere to confer dependable reinforcement for HVAC online governance.

The examination encompasses the construction of a database operating Computational Fluid Dynamics (CFD), verified by empiricals. The examination delineates comprehensive assessment indices to provide weighting constituents for indoor surroundings and air conditioning energy. The consequences exhibit the HVAC energy expenditure consequential from ventilation and air conditioning burdens could be significantly reduced up to 50% and 32%, respectively.

This study presents a comprehensive investigation into the thermodynamic performance of an integrated inverter split Air Conditioning (AC) system, leveraging microcontroller technology for enhanced monitoring and analysis. The research aims to contribute novelty to the field by offering detailed insights into various thermodynamic parameters crucial for system evaluation. The experimental setup involves the monitoring of key parameters including supply and return temperatures at the evaporator, as well as voltage, current, power and energy consumption across the cooling system. By precisely tracking these variables, the study seeks to provide a thorough understanding of the system's thermodynamic behavior under different operating conditions. To achieve precise and real-time monitoring, the research employs an advanced ATmega 2560 microcontroller. This microcontroller technology offers a significant improvement over traditional monitoring approaches, enabling more accurate and dependable data collection. By utilizing the capabilities of the microcontroller, the study enhances the reliability and robustness of the experimental measurements, facilitating a more comprehensive analysis of the integrated split AC system's thermodynamic performance.

2 Method

2.1 Experimental Setup of Investigation

A 2.5 kW capacity split inverter air conditioner was utilized in this experiment with specifications shown in Table 1. This air conditioning system used R410A refrigerant as the working fluid. The split inverter air conditioner was installed in the Refrigeration Mechanical Engineering laboratory at the Bali State Polytechnic for the experimental investigation. The primary components of the experimental setup included: the split inverter AC unit, laptop/ PC, ATmega2560 microcontroller, PZEM 004-T power meter, DS18B20 temperature sensor, SD card module, ammeter, project board, 20 × 4 I2C LCD display, and jumper cables. The ATmega2560 microcontroller offered advantages over the ATmega328P microcontroller[23]. This microcontroller was selected due to its superior ability to log data for each experiment in this study. As shown in Table 2[24], [25], the ATmega2560 has 54 digital input/output pins and 16 analog inputs. Furthermore, its expanded memory capacity compared to the ATmega328P enabled running multiple programs concurrently[26]. Arduino IDE software was installed to interface the microcontroller and sensors utilized in the investigation. An experimental schematic of the integrated inverter split Air Conditioning (AC) system with microcontroller technology is shown in Fig. 1.

Table 1. Technical details of split inverter air conditioner

Model	Refrigerant: R-410A	
	Unit	Values
Cooling		
Capacity	kW	2.5
Input power	kW	0.485
Rated current	A	2.7
Maximum power	kW	2.06
Maximum current	A	9.5
Compressor speed range	RPM	600–3600
Heating		
Capacity	kW	3.2
Input power	kW	0.58
Rated current	A	3
Maximum power	kW	2.06
Maximum current	A	9.5
Compressor speed range	RPM	600–3600

Table 2. Technical details of microcontroller [27]

Microcontroller	ATmega 2560 R3
Operating voltage	5V
Input voltage	6-20V
Digital I/O pins	54 of which provide PWM output
Analog input pins	16
DC current per I/O pins	20 mA
Flash memory	256 kB of which 8 kB used by bootloader
SRAM	8 kB
EEPROM	4 kB
Clock speed	16 MHz

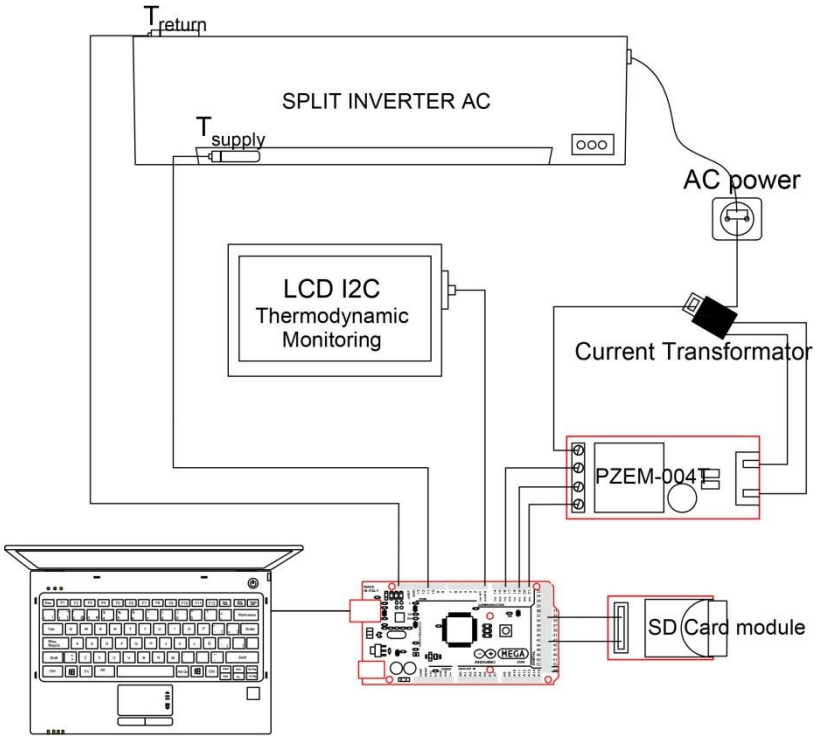

Fig. 1. Schematic diagram of the integrated inverter split air conditioning system with microcontroller technology.

A DS18B20 sensor was utilized to measure evaporator temperature during the investigation. This sensor has a measurement range from −55°C to 125°C with a specificity of ±0.5°C[28]. The DS18B20 sensors were positioned at the supply and return of the evaporator to quantify the range of evaporator temperature differences. The DS18B20 temperature sensors were equipped with a single 4.7KOhm resistor. A400-point solderless breadboard was employed in this study. To quantify electrical parameters including power, current, voltage, and energy consumption of the inverter split AC, a PZEM 004-T module was implemented. This module provides comprehensive electrical metrics and is available in 10 and 100 ampere models. The advantage of this module is the self-contained split core Current Transformer (CT) that can be directly installed on a power network[29]. The module output was connected to a current source while the CT was linked to the inverter split AC load to evaluate parameters in coordination with the ATmega 2560 microcontroller. A 20×4 I2C LCD screen displayed investigational readings. All major components were integrated with the microcontroller. Experimental testing targeted evaporator supply and return temperatures, current, voltage, power, and energy consumption. Remote temperatures of T1 (16°C), T2 (18°C), T3 (20°C), T4 (22°C), and T5 (24°C) were each evaluated in hour-long experiments and compared.

During the thermodynamic monitoring investigation of the split inverter AC, it was assumed that the room heat load remains constant. This assumption was foundational for ensuring the validity and reliability of the experimental conditions. By maintaining constant heat load throughout the investigation, any observed changes in system performance can be confidently attributed to the specific variables under examination, such as the operation of the AC unit itself. This control over the environmental conditions helps to isolate the effects of the AC system from external factors, allowing for a more precise analysis of its thermodynamic behavior. Thus, the assumption of a constant heat load serves as a critical element in revealing the complexities of the system's performance and its response to varying operational parameters.

2.2 Microcontroller Configuration for Sensor Integration

Fig. 2 shows the microcontroller configuration for each sensor utilized in the system. The DS18B20 digital temperature sensor contained a data pin, power (VCC), and ground (GND). Its data pin was interfaced to pin 7 of the ATmega 2560 microcontroller, with a 4.7KOhm pull-up resistor connected between the data and VCC lines. The PZEM-004T ACower monitor uses separate receive (RX) and transmit (TX) pins for UART serial communication, as well as VCC and GND connections. The I2C communication pins, serial clock (SCL) and serial data (SDA), of the Liquid Crystal Display (LCD) module are both connected to individual digital input/output pins on the ATmega 2560.

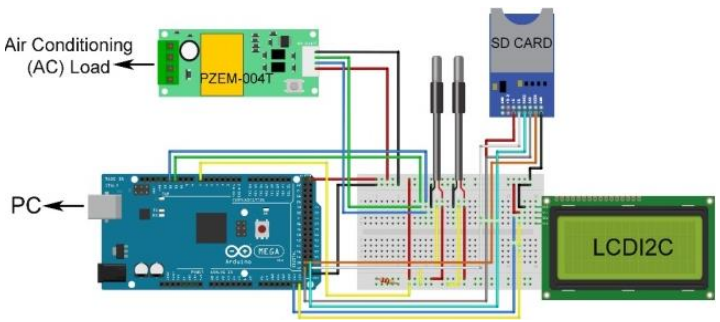

Fig. 2. Schematic of microcontroller configuration for each sensors.

The Secure Digital (SD) memory card interface module contains several connection pins, including Chip Select (CS), Master out Slave in (MOSI), serial clock (SCK), Master in Slave out (MISO), ground (GND), and positive supply voltage (VCC). For integration with the microcontroller, the CS pin was connected to digital I/O pin 53 of the ATmega 2560, the SCK pin was interfaced with pin 52, the MOSI and MISO pins were linked to digital pins 51 and 50, respectively. This wiring configuration all other ATmega 2560 microcontroller to communicate with the SD module using the Serial Peripheral Interface (SPI) protocol. The SPI bus provides full-duplex synchronous serial communication between the microcontroller as master and the SD card module as slave. By manipulating the CS pin and transferring serial data on MOSI and MISO in a time-coordinated fashion using the SCK clock, the ATmega 2560 can read and write data to the non-volatile storage on the SD card.

3 Results and Discussion

3.1 Thermodynamic Monitoring of Evaporator Temperature

Fig. 3 shows the thermodynamic monitoring of T_{supply}variation for each remote temperature. It is evident that all remote temperatures presented a precipitous drop of approximately 18°C around 300 s. Temperatures T4 and T5 decreased to 12.25°C at roughly 1250 s and remained relatively constant at 10.75°C from 2000 to 2900 s. However, both T4 and T5 declined slightly to 9.5°C and 10°C, respectively, around 3500 s. Furthermore, no significant temperature differential was observed between T4 and T5. Monitoring of T1 showed a decrease to 11.5°C followed by reductions in T2 to 12.5°C and T3 to 12.75°C at 600 s, attributable to the refrigerant evaporation process. Subsequently, the refrigerant underwent a phase transition to vapor and entered the compressor. At approximately 2500s, the temperatures were recorded as 8.75°C, 9.25°C, and 9.5°C for T1, T2, and T3, respectively. T2 and T3 exhibited similar trends with no major differences. Additionally, the minimum temperature reached 8°C at T1 around 3500 s and remained relatively constant for the duration of the study. From Fig. 3, it is evident that T1 trended lower than the other remote temperatures, while T5 remained relatively higher. This is because T1 represents the minimum remote temperature in the split inverter AC system [31]. In thermodynamics, the reason for this phenomenon lies in the operation of the air conditioning system. T1, being set as the lowest temperature within the system, plays a crucial role in absorbing significant quantities of warm room air. This absorption process occurs to facilitate the evaporation of the absorbed air in the evaporator unit. By absorbing the warm air from the room, T1 initiates the cooling process by evaporating this air in the evaporator, leading to a decrease in temperature within the AC system. This fundamental principle underscores how T1's function as the lowest temperature setting enables the system to efficiently cool the air by absorbing and evaporating warm room air in the evaporator unit [3]. In addition, T4 and T5 were comparatively higher in contrast to T1, T2, and T3, indicative of lower heat absorption in that room. Monitoring showed an inverse relationship between heat absorption and T_{supply} to the evaporator.

The variation of T_{return} for each remote temperature sensor is shown in Fig. 4. From the figure, the temperatures at all sensor positions decreased over an approximate 600 s duration. This phenomenon is attributable to the heat absorption by the evaporator and subsequent heat rejection to the ambient environment via the condenser [32]. To achieve a reduction in temperature, room heat must be absorbed by the evaporator to vaporize the refrigerant. The higher heat removal from the room enables lower achievable temperatures. Furthermore, temperatures T4 and T5 were observed to reduce to 26.75°C after 600 s. Subsequently, T4 decreased slightly to 25.75°C while T5 reached 26.25°C at approximately 3000 s. T3 was found to reduce to 25.75°C by 2400 s and remained relatively constant from 3000 s onward. The return temperature is primarily dependent on the cooling load in the given space. Higher cooling loads necessitate

greater return temperatures. The monitoring revealed T1 and T2 decreased identically to 25.75°C by 2400 s, with a small further reduction to 25.5°C at 3000 s. Both T1 and T2 exhibited comparable decreasing trends and remained relatively stable for the experiment duration. The return temperature closely aligns with the room temperature [33].

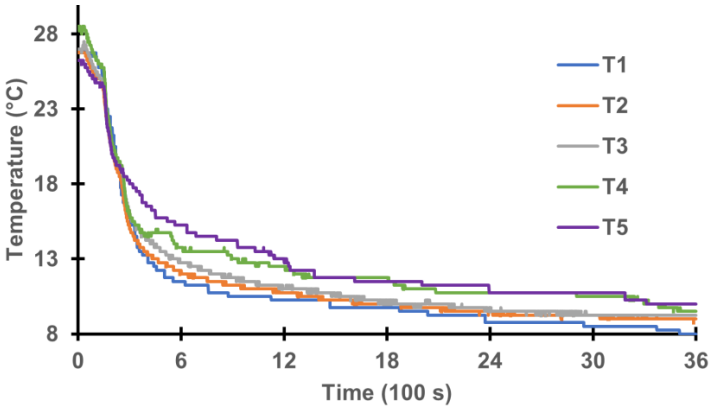

Fig. 3. Thermodynamic monitoring of T_{supply} variation for each remote temperature.

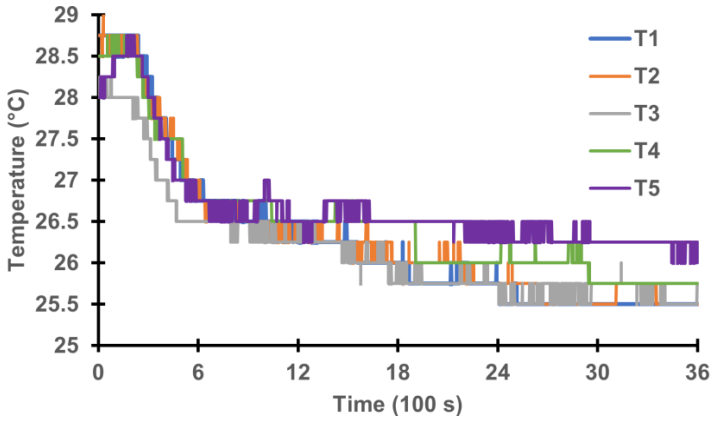

Fig. 4. Thermodynamic monitoring of T_{return} variation for each remote temperature.

3.2 Thermodynamic Monitoring of Electrical Parameters

Fig. 5 shows the voltage variation of each remote temperature sensor. Fluctuations in voltage are evident throughout the experiment. Specifically, at approximately 600 s, the measured voltages were 229.1 V, 226.7 V, 228 V, 224 V and 228.1 V for V1 through V5, respectively. A single-phase power distribution network was implemented for this investigation. Single-phase grids typically exhibit voltage ranges centered around 220-240 V. However, the results in Fig. 5 demonstrate the voltages remained within a consistent band aligned with standard single-phase electrical network parameters. The maximum and minimum recorded voltages were 231.2 V at V2 and 222.2 V at V4, in that order. These voltage variations can be attributed to fluctuations in electrical loading stemming from the room's energy usage over the experiment timeframe [34]. In addition, Fig. 5 provides insight into voltage behavior across a single-phase system powering a variable load, with the observed fluctuations highlighting the influence of electrical demand on overall grid voltage.The variation in electric current from each remote temperature is presented in Fig. 6. It can be observed that I1-I4 increase sharply up to approximately 3.8 A at 600 s. Subsequently, the electric current remained relatively constant for I1-I3 during the investigation with no discernible fluctuations. I1-I3 exhibited a tendency to be higher than the other currents. These results were consistent with the standard specifications for a split inverter air conditioner as shown in Table 1, which indicated a maximum output electric current of around 3.5 A. Slight fluctuations in I4 were observed from 1300 s to 2500 s. These minor variations are within acceptable limits given the expected range of currents for a split inverter air conditioner. Furthermore, I5 was notably lower compared to the other amperages. This is due to I5 corresponding to the highest remote temperature applied in this study. Fig. 6 also shows that the remote temperature is inversely related to the electric current. However, the electric current is also dependent on the particular specifications and performance of the split inverter air conditioner[35].

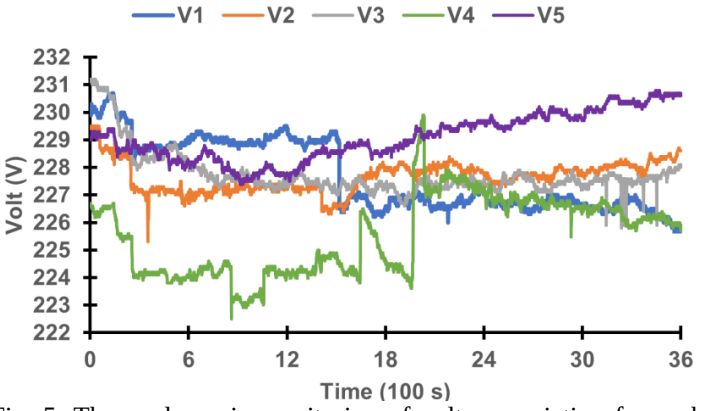

Fig. 5. Thermodynamic monitoring of voltage variation for each remote temperature.

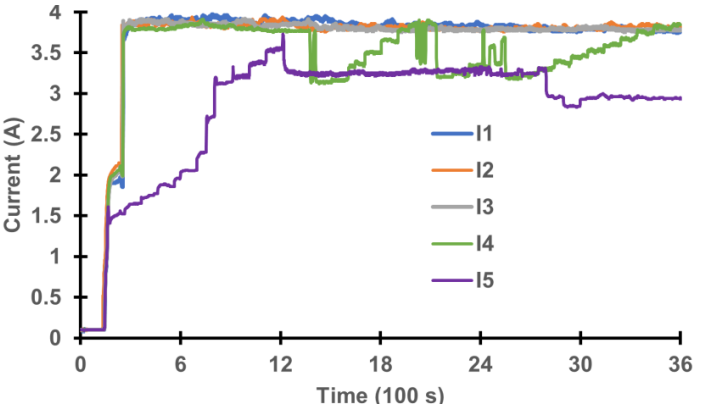

Fig. 6. Thermodynamic monitoring of electric current variation for each remote temperature.

Variations in power from each remote temperature are presented in Fig. 7. It can be observed that all power variables exhibit a considerable increase with rising investigation time up to 600 s, corresponding to the activation of the split inverter air conditioner. P1-P4 remained relatively constant up to 1200 s. However, P5 was notably lower compared to the other power measurements, attributable to the reduced electric current consumption. Power is dependent on both current and voltage[36]. Furthermore, no appreciable difference was discerned between P1-P3 during the study. At 2400 s, the power was measured as 792.2 W, 765.5 W, and 767.8 W for P1-P3, respectively. These results are consistent with the specifications for a 2.5 kW capacity split inverter air conditioner, indicating an average power consumption of approximately 750 W. This consistency highlights the reliability and adherence of the system to its rated capacity, indicative of its stable and efficient operation. Moreover, observations of P4 and P5 yielded readings of 657.5 W and 624.3 W, respectively, which were notably lower than those of P1-P3. This difference may signify variations in system load or efficiency across different components or operating conditions. Notably, a minor fluctuation in P4 was detected between 1300 and 2400 s, following which P4 displayed an upward trend with increasing investigation time. This temporal evolution could be attributed to dynamic changes in ambient conditions, system dynamics, or other external factors influencing the performance of the air conditioning unit. The incremental trend observed in P4 highlights the dynamic nature of the system's power consumption behavior

over time, suggesting a potential correlation between investigation duration and energy usage[32].

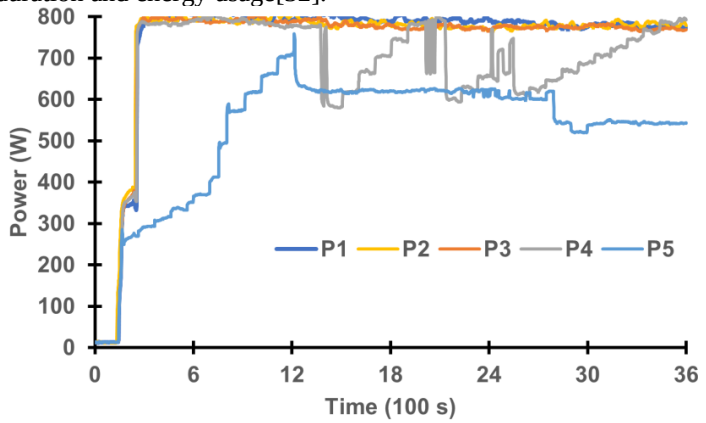

Fig. 7. Thermodynamic monitoring of power variation for each remote temperature.

Fig. 7 also shows the direct proportionality between power and amperage for the split inverter air conditioner. As current increases, the power consumption of the AC likewise increases. This aligns with the fundamental relationship defining power as being dependent on both voltage and current. Variations in current were the primary factor driving changes in AC power, as the voltage was held constant. The influence of supply air temperature on power consumption is also evidenced in Fig. 3 and Fig. 7. The minimum AC supply temperature of T1 corresponded with the maximum power consumption of P1. This inverse correlation arises from the increased power required to achieve greater temperature reductions. Thermodynamically, larger heat transfer and thus higher power is necessitated to obtain lower supply air temperatures. Overall, the data definitively demonstrates an inverse proportionality between supply air temperature and power consumption of the split inverter AC under the tested conditions.

The energy consumption from each remote temperature sensor is shows in Fig. 8. From the figure, the energy consumption of E1-E3 exhibits a considerable rise with increasing investigation time. The energy consumption of E4 and E5 displays a relatively lower escalation. At approximately 600 s, the energy consumption is measured to be 0.11 kWh for E1-E4, while E5 exhibits an energy consumption of 0.04 kWh. E5 demonstrated the minimum energy consumption throughout the investigation, owed to its relatively lower power demand and current draw compared to the other parameters. This outcome is influenced by the current and power characteristics[37]. Negligible differences were observed among E1-E3, likely due to their relatively elevated current consumption and power demand. Furthermore, E4 showed slightly lower energy usage than E1-E3 but marginally higher than E5. Over the hour-long investigation, the maximum energy consumption peak of 0.96 kWh was attained at parameter E1.

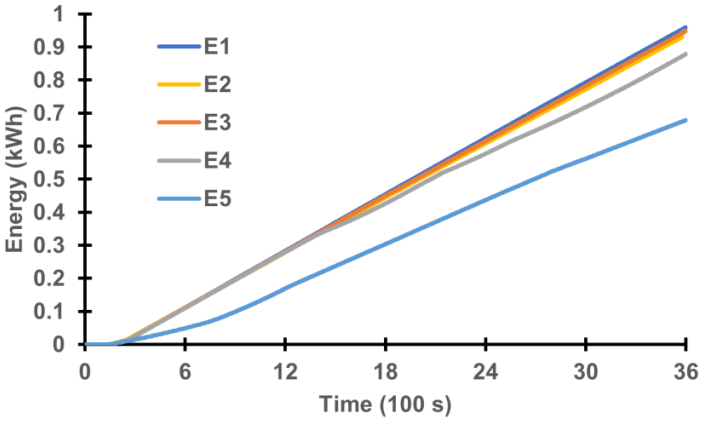

Fig. 8. Thermodynamic monitoring of energy consumption variation for each remote temperature.

Furthermore, Fig. 8 shows the relationship between energy consumption and temperature, current, and power. An inverse correlation is evidenced between energy consumption and temperature-heightened energy usage corresponds with decreased supply and return temperatures. Conversely, a direct proportionality exists between energy consumption, current and power. The higher the power consumption, the higher the current and power required by the AC split inverter. Variations in electrical consumption parameters with a fixed cooling load arise from disparities in remote temperature. In monitoring temperature, the supply temperature reflects evaporator temperature for room thermal comfort. Moreover, the supply and return temperature differential reaches 15°C. These results indicate effective return temperature reduction by the split inverter AC congruent with the remote temperature setpoint. Additionally, microcontroller-based testing enables acquisition of real-time experimental data with monitoring at 1-second intervals. This technology confers multiple advantages for investigating split inverter AC performance. The microcontroller has proven a promising technology for experimental thermodynamic monitoring based on the investigation results. In addition, affordability and portability render this technology well-suited for AC performance research and real-time data collection.

4 Conclusion

This study presents thermodynamics real-time monitoring of an air conditioning split inverter system utilizing microcontroller technology. The split inverter air conditioner under investigation has a rated capacity of 2.5 kW. Experimental observations reveal that the T_{supply} reached a minimum of 8°C for T1 (16°C) in comparison to other temperatures measured remotely. The reason for this phenomenon lies in the operation of the air conditioning system. T1, being set as the lowest temperature within the system, plays a crucial role in absorbing significant quantities of warm room air. Average power consumption of approximately 750 W corresponds to the rated capacity of the 2.5 kW inverter AC unit under study. The measured power consumption of 750 W falls within the anticipated range, indicating that the system is efficiently utilizing electrical energy to provide cooling.

This correspondence between observed and rated power consumption affirms the proper functionality of the AC system. It suggests that the components and mechanisms within the unit, including the compressor, evaporator, and inverter technology, are functioning as intended, resulting in the efficient conversion of electrical energy into cooling output. The energy consumption of E1-E3 exhibits a considerable rise with increasing investigation time. This escalating pattern suggests a direct correlation between lower temperatures and higher energy demand, indicating that the air conditioning system expends greater energy resources to maintain cooler indoor environments over extended periods.

Overall, the utilization of microcontroller instrumentation for real-time thermodynamic performance monitoring represents a significant advancement investigation methods, offering enhanced precision and data acquisition capabilities. This research highlights the effectiveness of the ATmega 2560 microcontroller as a versatile and reliable technology for probing the intricacies of AC cooling systems. The potential of the ATmega 2560 microcontroller to serve as the foundation for intelligent control systems opens up new avenues for innovation in the field of HVAC technology. By leveraging real-time data insights and adaptive control strategies enabled by the microcontroller, future AC systems can be designed to dynamically adjust operation parameters in response to changing environmental conditions, user preferences, and energy availability.

Acknowledgement

The authors acknowledge the financial support received from P3M of Bali State Polytechnic Indonesia.

References

[1] R. Santosh, G. Kumaresan, S. Selvaraj, T. Arunkumar, and R. Velraj, "Investigation of humidification-dehumidification desalination system through waste heat recovery from household air conditioning unit," *Desalination*, vol. 467, no. May, pp. 1–11, 2019, doi: 10.1016/j.desal.2019.05.016.

[2] A. A. M. Omara and A. A. A. Abuelnour, "Improving the performance of air conditioning systems by using phase change materials: A review," *Int. J. Energy Res.*, vol. 43, no. 10, pp. 5175–5198, 2019, doi: 10.1002/er.4507.

[3] S. I D. M. C., W. I N. G. S., S. P. W., and W. I G. A. B., "Investigation of optimization of solar energy refrigerator with natural humidifier," *Int. J. Thermofluid Sci. Technol.*, vol. 8, no. 2, 2021, doi: 10.36963/ijtst.2021080201.

[4] M. Kong, B. Dong, R. Zhang, and Z. O'Neill, "HVAC energy savings, thermal comfort and air quality for occupant-centric control through a side-by-side experimental study," *Appl. Energy*, vol. 306, no. PA, p. 117987, 2022, doi: 10.1016/j.apenergy.2021.117987.

[5] Q. Li, Y. Zhao, Y. Yang, L. Zhang, and C. Ju, "Demand-Response-Oriented Load Aggregation Scheduling Optimization Strategy for Inverter Air Conditioner," *Energies*, vol. 16, no. 1, pp. 1–15, 2023, doi: 10.3390/en16010337.

[6] I. G. A. Negara, A. A. N. B. Mulawarman, I. G. Santosa, and L. P. I. Midiani, "Studi Eksperimental Generator Elektrik Berbahan Bakar Biogas Guna Mendukung Net Zero Emission," vol. 14, no. 2, pp. 689–700, 2023, doi: 10.21776/jrm.v14i2.1431.

[7] I. G. A. Negara *et al.*, "Experimental Study of Cooling Performance and Electrical Parameters in a Microcontroller-Driven Inverter AC System," vol. 23, no. 2, pp. 81–90, 2023.

[8] Q. Al-Yasiri, M. Szabó, and M. Arıcı, "A review on solar-powered cooling and air-conditioning systems for building applications," *Energy Reports*, vol. 8, pp. 2888–2907, 2022, doi: 10.1016/j.egyr.2022.01.172.

[9] P. Zi *et al.*, "Modeling method of variable frequency air conditioning load," *Energy Reports*, vol. 9, pp. 1011–1017, 2023, doi: 10.1016/j.egyr.2022.11.035.

[10] M. Alawadhi and P. E. Phelan, *Review of Residential Air Conditioning Systems Operating under High Ambient Temperatures*, vol. 15, no. 8. 2022. doi: 10.3390/en15082880.

[11] H. Krishnaswamy, S. Muthukrishnan, S. Thanikodi, G. A. Arockiaraj, and V. Venkatraman, "Investigation of air conditioning temperature variation by modifying the structure of passenger car using computational fluid dynamics," *Therm. Sci.*, vol. 24, no. 1PartB, pp. 495–498, 2020, doi: 10.2298/TSCI190409397K.

[12] L. Belussi *et al.*, "A review of performance of zero energy buildings and energy efficiency solutions," *J. Build. Eng.*, vol. 25, no. December 2018, 2019, doi: 10.1016/j.jobe.2019.100772.

[13] S. Liu, S. Schiavon, H. P. Das, M. Jin, and C. J. Spanos, "Personal thermal comfort models with wearable sensors," *Build. Environ.*, vol. 162, pp. 0–34, 2019, doi: 10.1016/j.buildenv.2019.106281.

[14] Q. Zhao, Z. Lian, and D. Lai, "Thermal comfort models and their developments : A review," *Energy Built Environ.*, vol. 2, no. 1, pp. 21–33, 2021, doi: 10.1016/j.enbenv.2020.05.007.

[15] M. Babiuch, P. Foltynek, and P. Smutny, "Using the ESP32 microcontroller for data processing," *Proc. 2019 20th Int. Carpathian Control Conf. ICCC 2019*, no. May 2019, 2019, doi: 10.1109/CarpathianCC.2019.8765944.

[16] J. Park, R. A. Martin, J. D. Kelly, and J. D. Hedengren, "Benchmark temperature microcontroller for process dynamics and control," *Comput. Chem. Eng.*, vol. 135, 2020, doi: 10.1016/j.compchemeng.2020.106736.

[17] A. Latif, H. A. Widodo, R. Rahim, and K. Kunal, "AC of line follower robot based microcontroller atmega32a," *J. Robot. Control*, vol. 1, no. 3, pp. 70–74, 2020, doi: 10.18196/jrc.1316.

[18] S. Bipasha Biswas and M. Tariq Iqbal, "Solar Water Pumping System Control Using a Low Cost ESP32 Microcontroller," *Can. Conf. Electr. Comput. Eng.*, vol. 2018-May, 2018, doi: 10.1109/CCECE.2018.8447749.

[19] A. H. T. E. De Silva, W. H. P. Sampath, N. H. L. Sameera, Y. W. R. Amarasinghe, and A. Mitani, "Development of a novel telecare system, integrated with plantar pressure measurement system," *Informatics Med. Unlocked*, vol. 12, no. July, pp. 98–105, 2018, doi: 10.1016/j.imu.2018.07.001.

[20] K. Sumeru, T. P. Pramudantoro, and A. Setyawan, "Experimental investigation on the performance of residential air conditioning system using water condensate for subcooling," vol. 08002, 2018.

[21] Q. Deng, D. Liu, and Z. Zhou, "The effect of air-conditioner operation modes on the energy-saving capacity of external wall insulation in residential buildings," 2021, doi: 10.1177/0144598719895821.

[22] C. Ren and S. J. Cao, "Development and application of linear ventilation and temperature models for indoor environmental prediction and HVAC systems control," *Sustain. Cities Soc.*, vol. 51, no. July, 2019, doi: 10.1016/j.scs.2019.101673.

[23] A. S. Ismailov, "Study of arduino microcontroller board," *Sci. J.*, vol. 3, no. 3, pp. 172–179, 2022.

[24] L. Parra, S. Viciano-Tudela, D. Carrasco, S. Sendra, and J. Lloret, "Low-Cost Microcontroller-Based Multiparametric Probe for Coastal Area Monitoring," *Sensors*, vol. 23, no. 4, 2023, doi: 10.3390/s23041871.

[25] N. Kanti, D. Saha, and K. Biswas, "Smart Trash Collection System – An IoT and Microcontroller-Based Scheme," *J. Eng. Res. Reports*, vol. 24, no. 11, pp. 1–13, 2023, doi: 10.9734/JERR/2023/v24i11849.

[26] M. Khairudin *et al.*, "Temperature control based on fuzzy logic using atmega 2560 microcontroller," *J. Phys. Conf. Ser.*, vol. 1737, no. 1, 2021, doi: 10.1088/1742-6596/1737/1/012044.

[27] I. A. Adeyanju, S. O. Alabi, A. O. Esan, B. A. Omodunbi, O. O. Bello, and S. Fanijo, "Design and prototyping of a robotic hand for sign language using locally-sourced materials," *Sci. African*, vol. 19, p. e01533, 2023, doi: 10.1016/j.sciaf.2022.e01533.

[28] Ramesh Saha, S. Biswas, S. Sarmah, S. Karmakar, and P. Das, "A Working Prototype Using DS18B20 Temperature Sensor and Arduino for Health Monitoring," *SN Comput. Sci.*, vol. 2, no. 1, pp. 1–21, 2021, doi: 10.1007/s42979-020-00434-2.

[29] S. George and G. B, "IoT Based Smart Energy Management System using Pzem-004t Sensor & Node MCU," *Int. J. Eng. Res. Technol.*, vol. 9, no. 7, pp. 45–48, 2021.

[30] M. Setiyo, B. Waluyo, P. Gobbato, and M. Masi, "Energy efficiency ratio (EER) of novel air conditioning system on LPG fuelled vehicle: A lab-scale investigation," *Int. J. Automot. Mech. Eng.*, vol. 16, no. 3, pp. 7133–7143, 2019, doi: 10.15282/ijame.16.3.2019.21.0533.

[31] E. O'Shaughnessy, D. Cutler, K. Ardani, and R. Margolis, "Solar plus: Optimization of distributed solar PV through battery storage and dispatchable load in residential buildings," *Appl. Energy*, vol. 213, pp. 11–21, 2018, doi: 10.1016/j.apenergy.2017.12.118.

[32] Y. Heredia-Aricapa, J. M. Belman-Flores, A. Mota-Babiloni, J. Serrano-Arellano, and J. J. García-Pabón, "Overview of low GWP mixtures for the replacement of HFC refrigerants: R134a, R404A and R410A," *Int. J. Refrig.*, vol. 111, pp. 113–123, 2020, doi: 10.1016/j.ijrefrig.2019.11.012.
[33] L. Zhou *et al.*, "A polydimethylsiloxane-coated metal structure for all-day radiative cooling," *Nat. Sustain.*, vol. 2, no. 8, pp. 718–724, 2019, doi: 10.1038/s41893-019-0348-5.
[34] E. S. Jun, S. Y. Park, and S. Kwak, "Model predictive current control method with improved performances for three-phase voltage source inverters," *Electron.*, vol. 8, no. 6, 2019, doi: 10.3390/electronics8060625.
[35] A. Rahman, "Mitigation of Single Phase Voltage Sag, Swell and Outage Using Voltage Controlled Voltage Source," *Glob. Sci. J.*, vol. 7, no. 10, 2019.
[36] G. Pan, W. Gu, Y. Lu, H. Qiu, S. Lu, and S. Yao, "Optimal Planning for Electricity-Hydrogen Integrated Energy System Considering Power to Hydrogen and Heat and Seasonal Storage," *IEEE Trans. Sustain. Energy*, vol. 11, no. 4, pp. 2662–2676, 2020, doi: 10.1109/TSTE.2020.2970078.
[37] Y. Kassem, H. Çamur, and R. A. F. Aateg, "Exploring solar and wind energy as a power generation source for solving the electricity crisis in Libya," *Energies*, vol. 13, no. 14, 2020, doi: 10.3390/en13143708.